

Article

Dominance Patterns Specified by the Ideal Gas Equation: Example of Examining Simultaneous Multivariate Relation with Scale Analysis Approach

Juqing Tu ^{1,2}, Dian Yuan ² and Er Lu ^{2,*}¹ School of Geographic Information and Tourism, Chuzhou University, Chuzhou 239000, China² Key Laboratory of Meteorological Disaster, Ministry of Education (KLME), Joint International Research Laboratory of Climate and Environment Change (ILCEC), Collaborative Innovation Center on Forecast and Evaluation of Meteorological Disasters (CIC-FEMD), Nanjing University of Information Science and Technology, Nanjing 210044, China

* Correspondence: elu@nuist.edu.cn

Abstract: Climate science involves various functional relations and needs to investigate the dominance or relative importance of the variables in their relation. In our previous studies, we examined several problems in which causal relations are established, showing how the dependent quantity is affected by two or more independent variables. With linear fitting, the relative contributions of the variables to the variation of the quantity are compared. In this study, we examine constraint relation, which is a simultaneous multivariate relation, with all variables in the relation being equal in position. The relation can generally be nonlinear. To be convenient for examining the dominance, plane equation fitting can be used to linearize the relation. The equation of state for ideal dry air is investigated as a simple case of the relation. For this special case, a linearized relation can be obtained from both the fitting and the derivation. The scale analysis tool used in dynamic meteorology is applied here for the dominance analysis. Through comparing the scales of the terms, we can simplify the equation. The simplified relations correspond, respectively, to Charles's law, Boyle's law, and Gay-Lussac's law. The geographical preferences of the different dominance patterns are exhibited. In addition, when considering the change of the variable that is smallest in scale, we can identify which factor is the dominator. The ideal gas law is intentionally chosen as the example, since the relation is simple in form, and the results of dominance can be deduced analytically. A comparison demonstrates that the methods used here for the dominance analysis are reliable.

Keywords: dominance; nonlinear; multivariate; scale analysis; ideal gas law

Citation: Tu, J.; Yuan, D.; Lu, E. Dominance Patterns Specified by the Ideal Gas Equation: Example of Examining Simultaneous Multivariate Relation with Scale Analysis Approach. *Atmosphere* **2023**, *14*, 293. <https://doi.org/10.3390/atmos14020293>

Academic Editor: Santtu Mikkonen

Received: 30 October 2022

Revised: 28 January 2023

Accepted: 30 January 2023

Published: 1 February 2023



Copyright: © 2023 by the authors. Licensee MDPI, Basel, Switzerland. This article is an open access article distributed under the terms and conditions of the Creative Commons Attribution (CC BY) license (<https://creativecommons.org/licenses/by/4.0/>).

1. Introduction

Quantitative studies in climate science involve various functional relations. They may include the statistically established relations, e.g., the prediction of precipitation with preceding sea surface temperature and snow cover over the Tibetan Plateau, along with other possible factors. The functional relations include the physical laws, e.g., the equation of state for ideal dry gas, which provides a linkage among atmospheric pressure, density, and temperature. The functional relations may also include those that are mathematically defined based on physical considerations, e.g., the link of relative humidity with atmospheric water vapor and air temperature.

These functional relations can be classified into two types. One is the causal relation, in which a dependent quantity is affected by two or more independent variables, as in the example of using sea surface temperature and the snow cover over the plateau to predict the precipitation. The other type is the constraint relation. As a simultaneous relation, it includes three or more variables in an equation. There is no causality, and all the variables are equal in position. The ideal gas law is an example of this type. The relation

of relative humidity, water vapor, and air temperature can be treated as a causal relation when examining how water vapor and air temperature influence relative humidity. It may also be treated as a constraint relation, as in meteorological calculation when computing one of the humidity quantities with the data of the other two variables.

Dominance analysis [1,2] can be performed with quantitative relations to better understand the corresponding issues. For causal relations, we can compare the relative contributions from the independent variables to the variation of the dependent quantity and identify which variable is more important to the variation. Lu et al. [3] studied the interannual variations of streamflow and other hydrological components and examined whether precipitation or temperature, the two input climate variables, dominates the variations. Lu et al. [4] investigated the interannual variation of the seasonal rainfall total, with different thresholds for defining the precipitation and explored whether the number of rainy days or the averaged rainfall intensity dominates the variation. Precipitation can be affected by changes in atmospheric water vapor and air temperature, which can both be influenced by atmospheric circulation. Tu and Lu [5] revealed whether the change in water vapor or the change in air temperature is more important to the interannual variation of seasonal precipitation. Derivation shows that the atmospheric static stability is a function of air temperature and its vertical difference. Lu et al. [6] provided the results of whether temperature or the vertical difference of temperature is more important to the seasonal, interannual, and spatial variations of the static stability. In the present study, we turn to examining the constraint relation. As an example, here we consider the ideal gas law [7] and investigate the pertinent dominance issues.

Broadly speaking, all quantitative relations can be treated as nonlinear relations. For the dominance analysis, it would be convenient if the relations can be linearized. With observed data, statistical fitting can be used to obtain the linear relations. Significance tests are required to ensure the robustness of the linearization. Previous studies showed that for many of the problems examined, statistical fittings could well linearize the corresponding relations [1–6,8]. For the different causal relations, the independent variables are regressed with respect to the dependent quantity [3–6]. In this study, for the constraint relation, the linearization of the relation will be performed by using the plane equation fitting [9–13], in which the noise may come from all the variables. The advantage of the plane equation is that the relation fitted can cover all the situations, including those degenerate cases, i.e., the special cases with the simplified relations being between different pairs of the variables.

In the fitted plane equation, the dominance can be examined by using the “scale analysis”, which is a powerful tool in mathematical sciences for simplifying equations that contain multiple terms [14–18]. The method has conventionally been used in dynamic meteorology for analyzing the balance equations, such as the conservations in momentum, mass, and energy [19–21]. In the present study, through linearization, we establish a balance equation that has three terms. Because of the normalizations, the changes of the different variables can be compared. The scales of the three terms can be measured simply with the three coefficients contained in the linearized equation. For this specific gas law issue, a linearized relation can be obtained from both statistical fitting and analytical derivation.

With the balance equation of the three terms, the dominance analysis includes two aspects. One is simplifying the equation. With neglecting the term that is smallest in scale, the equation can be simplified as a rough balance between the other two terms. The three types of the simplifications can reflect the three ideal gas laws, that is, Charles’ law, which states that when pressure does not change, the density is inversely proportional to temperature [22], Boyle’s law, with temperature remaining unchanged and density being proportional to pressure [23], and Gay-Lussac’s law, in which density is constant while pressure is proportional to the temperature [24]. The other aspect of dominance analysis is to locate the dominant quantity when examining the variation of the term that is smallest in scale. The term is a residual between the two larger terms. The largest term dominates the variation, while the second largest term exerts a negative effect on the variation. For

the different dominance types and patterns, their geographical preferences are revealed in this study.

The equation of state for ideal dry air provides a nonlinear and simultaneous multivariate relation. The physical relation of the three quantities, as an equation, is simple in form. While we determine the dominance quantitative by use of the calculation approach, we may also deduce the dominance analytically from the original physical relation. Thus, their results can be compared. This is the reason why we deliberately choose the ideal gas law as the example for the dominance analysis. The comparison demonstrates that the approach used for the study is reliable.

Atmospheric pressure, temperature, and density are important climate quantities. They can both influence and be influenced by the atmospheric circulation. The spatial inhomogeneity of the pressure, as well as the high and low pressure systems, can affect the regional and large-scale circulations [25–28]. The horizontal difference of air temperature may lead to thermal wind and jet streams [29–32]. The temporal–spatial variations of the air density may relate to the convergence of the air parcel and then the wind energy, the gravity waves, and the greenhouse temperature [33–37]. In this study, we focus on the interannual variations of the near-surface atmosphere.

The NCEP/NCAR Reanalysis I [38], provided by the National Centers for Environmental Prediction (NCEP) and the National Center for Atmospheric Research (NCAR), is used in this study. The data used include the monthly surface air temperature and pressure, with a horizontal resolution of $2.5^\circ \times 2.5^\circ$ in latitude and longitude over the 71 years from 1948 to 2018. The monthly surface air density is then calculated with the ideal gas law.

The main goal of the present study is to raise the question, propose the method, and take the state equation of dry air near surface as an example to locate the regions, over the globe where the relation of the three quantities is dominated by the different types and patterns. In Section 2, plane equation fitting is applied, as for the general nonlinear problem, to linearize the relation. In addition, for this special problem, the gas law, the linear relation is also obtained from the derivation. In Section 3, we assess the relative importance for each pair of the quantities through comparing their coefficients obtained in the linearized relation. In Section 4, comparisons are further performed among the three coefficients to display the regional patterns for the dominance. The scale analysis tool is introduced to simplify the three-quantity equation and determine the dominant relation and the dominant quantity. An example is provided in Section 5, for the most common pattern, to present the details pertinent to the coefficients and the scales and the correlations and the normalizations, as well as the balance of the terms in the equation and their interannual variations. A summary and discussion are given in Section 6.

2. The Linearized Relation and the Coefficients

2.1. The Linear Fitting as a General Nonlinear Problem

Consider a general relation $F(X, Y, Z) = 0$, in which the three quantities X , Y , and Z are nonlinearly linked. If they are simultaneous variables and there is no definite causality among them, we may not simplify the relation, say, as $Z = f(X, Y)$, which defines X and Y as independent variables and Z as a dependent quantity. For the general nonlinear relation, we may use a statistical fitting, i.e., the plane equation $aX + bY + cZ + d = 0$, to linearize the relation. By using the data sampled from the variations of the three quantities, the plane fitting is performed with the total least squares (TLS) method [9,11,13,27]. It minimizes the total squares of the distance from each sample point to the fitted plane, with the constraint $a^2 + b^2 + c^2 = 1$.

The gas law is a nonlinear relation, though it is simple in form. The above linear fitting method that is for the general nonlinear problem is used here, as an example, to linearize the gas law. Denote the monthly surface air pressure, density, and the thermodynamic temperature in kelvins as p , ρ , and t , respectively. With the data from the interannual covariations, we first normalize the three quantities, which makes it easy to compare the changes of the different quantities. Denote the normalized monthly surface air

pressure, density, and temperature as P , D , and T , respectively. Namely, $P = (p - \bar{p})/\sigma_p$, $D = (\rho - \bar{\rho})/\sigma_\rho$, and $T = (t - \bar{t})/\sigma_t$, where \bar{x} and σ_x are the average and standard deviation of the x calculated from the data of the interannual variations.

Because of the normalizations, the constant term, i.e., the last term on the left side of the plane equation, tends to be zero. So, the plane equation fitted can finally be written as

$$A_D D + B_T T - C_P P = 0. \tag{1}$$

Here, we use the prescription $C_P > 0$. With this, the signs of A_D and B_T are then to be determined. We also use the constraint relation $A_D^2 + B_T^2 + C_P^2 = 1$. The plane fitting, i.e., the calculation of the three coefficients A_D , B_T , and C_P , is performed for each month and for every grid point over the globe, by using the monthly data of the 71 years.

Significance tests are required to ensure the validation of the fitted linear relation. Here, we use the coefficient of determination or the multiple-correlation coefficient [12], as applied in [5]. Figure 1a,b show the distributions of the correlation for January and July between the P calculated with the observed data and the P calculated with the relation obtained from the plane fitting. The correlation coefficient is over 0.95 across the entire field and is over 0.99 in almost all the grid points. This suggests the robustness of the linearization, and the plane fitting of the relation is perfect everywhere.

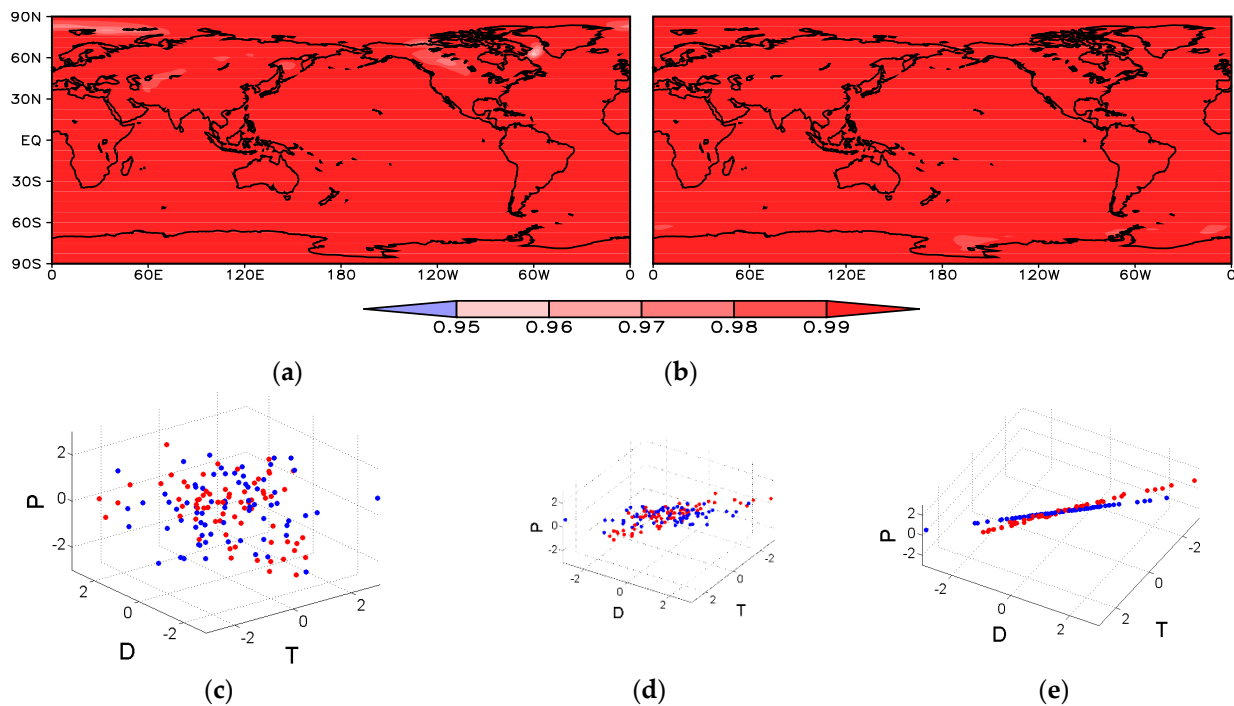


Figure 1. Distributions of the correlation between the surface air pressure observed and the surface air pressure calculated with the relation obtained from the plane fitting for (a) January and (b) July, and (c–e) the three-dimensional scatter plots for January (blue) and July (red) with the three dimensions being the normalized surface air pressure (P), density (D), and temperature (T) and the data from a grid point (90° E, 35° N) in the Tibetan Plateau. In plots (c–e), samples are viewed from different angles.

Figure 1c–e show, as an example to display the plane fitted, the three-dimensional scatter plots for a grid point (90° E, 35° N) over the Tibetan Plateau. In the space of the D , T , and P , the scattered points represent the samples from 71 years. The three plots are viewed from different angles, showing that gradually the view of these points can tend to be a plane. In the last plot, which is from a specific angle, the points appear approximately as a line, which actually represents a plane. The planes obtained for January and July are slightly different.

Figure 2 presents the distributions of the coefficients A_D , B_T , and C_P for six selected months. It is shown that in the fitted plane equation, corresponding to the prescribed positive value for the C_P , the A_D and B_T determined from the fitting are both positive for all the grid points in the globe and for all the months. As will further be analyzed in Sections 4 and 5, the normalizations of the three quantities imply that they are all the in magnitude of one. So, the magnitudes of the three terms in the equation, $A_D D$, $B_T T$, and $C_P P$, can be reflected with the coefficients A_D , B_T , and C_P .

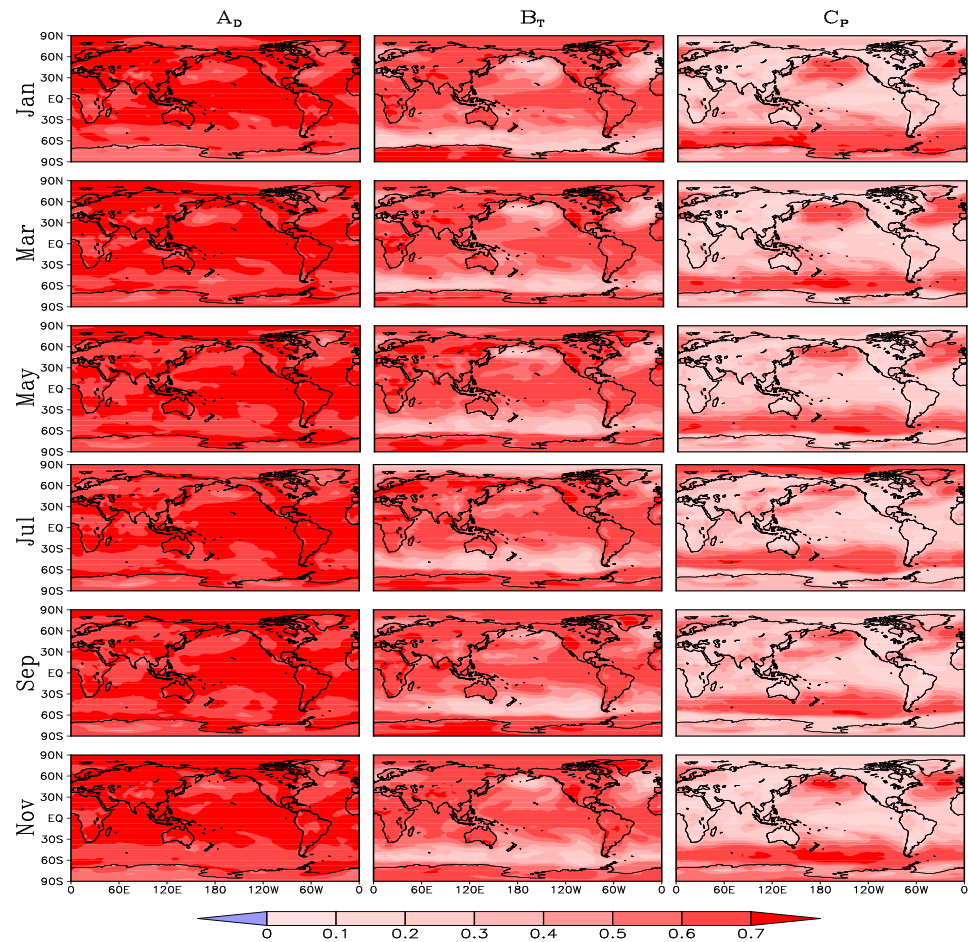


Figure 2. Distributions of the coefficients A_D (left), B_T (middle), and C_P (right) obtained from the plane fitting, for the six selected months.

2.2. The Linear Relation Derived for This Specific Problem

For this special problem, the gas law, we may obtain a linearized relation through derivations. With the monthly quantities, the equation of state for dry air is

$$p = \rho R t, \tag{2}$$

where R is the gas constant for dry air. The state with the averages of the three quantities can also satisfy the gas law, i.e., $\bar{p} = \bar{\rho} \cdot R \cdot \bar{t}$, considering that the eddy effect between the density and temperature is very small. With these, as derived in dynamic meteorology [27], we obtain the linear relation

$$(p - \bar{p})/\bar{p} = (\rho - \bar{\rho})/\bar{\rho} + (t - \bar{t})/\bar{t}. \tag{3}$$

By using the normalized quantities and the standard deviations, the equation can be expressed as

$$a'D + b'T - c'P = 0, \tag{4}$$

where $a' = \sigma_\rho / \bar{\rho}$, $b' = \sigma_t / \bar{t}$, and $c' = \sigma_p / \bar{p}$. Through normalizing the three coefficients, we finally obtain

$$A'_D D + B'_T T - C'_P P = 0, \tag{5}$$

where A'_D , B'_T , and C'_P are the ratios of the a' , b' , and c' , respectively, to the $\sqrt{a'^2 + b'^2 + c'^2}$.

Results indicate that Equation (4) is exactly the same as Equation (1). We also plot the distributions of the coefficients A'_D , B'_T , and C'_P for the six selected months (figures not shown). Comparisons show that the plots of these coefficients are, accordingly, the same as the plots of the coefficients A_D , B_T , and C_P . We cannot perceive any difference between the A'_D and A_D , the B'_T and B_T , and the C'_P and C_P in their global distributions of each month.

3. The Comparisons between Each Pair of the Coefficients

Figure 3 shows the distributions of the ratios B_T/A_D , A_D/C_P , and B_T/C_P for the six months. The plots of B_T/A_D illustrate the relative importance of the temperature and density in the covariations. At most grid points in the globe, A_D is larger than B_T throughout the year, especially at the belts over the mid-high-latitude oceans in the two hemispheres. Thus, density is more important than temperature in the covariations. However, in some areas, e.g., Central Africa, northern Eurasia, the Tibetan Plateau, the West Coast of North America, Greenland, and Antarctica, the B_T in some months can be larger than A_D , thus temperature is more important than density. The spatial pattern of the B_T/A_D also has seasonal shifts, and this is mainly due to the significant seasonal shifts of the B_T , along with the smaller seasonal changes in the A_D .

The plots of A_D/C_P compare the contributions of density and pressure. The A_D is larger than C_P in most regions over the globe, especially over the lands and the tropical and subtropical oceans, throughout the year. Hence, overall density is more important than pressure in the covariations. The plots of B_T/C_P compare the contributions of temperature and pressure. The general spatial pattern of B_T/C_P is similar with that of A_D/C_P . The difference is that in the plots of B_T/C_P , there are large areas where C_P is larger, e.g., over the mid-high-latitude oceans in the two hemispheres. This may be associated with the storm track in the middle latitudes, where the variations in pressure are relatively large, while sea surface temperature (and hence surface air temperature) varies rather little. In both the plots of A_D/C_P and B_T/C_P , seasonal shifts can be noticed for the belts in the two hemispheres, where correspondingly, the C is larger.

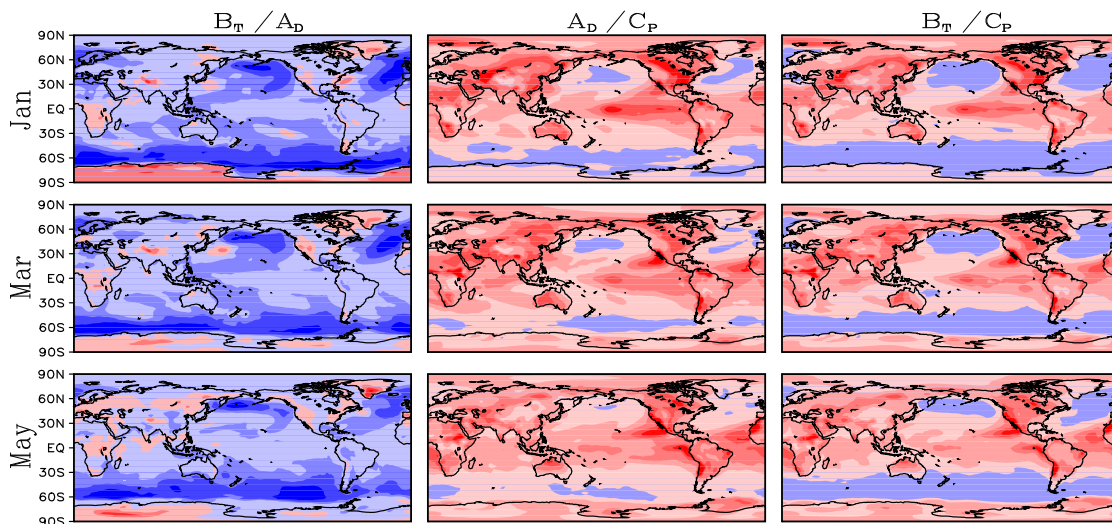


Figure 3. Cont.

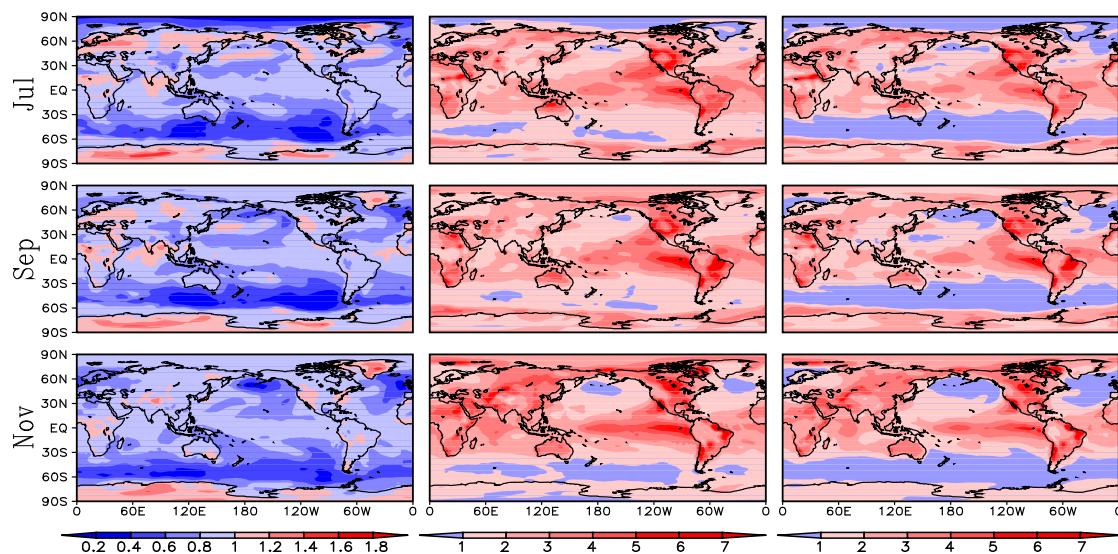


Figure 3. Distributions of the ratios (left), A_D/C_P (middle), and B_T/C_P (right), for the six months.

4. Scale Analysis of the Balance Equation and Regional Dominance of the Relation

4.1. The Scales and Dominance Issues for the Three-Quantity Equation

Scale analysis, or the order-of-magnitude analysis, is a useful tool for the simplification of an equation that contains multiple terms. It first approximates the magnitude of each individual term in the equation and then neglects some small terms and thus simplifies the equation. The scale analysis method has been applied in dynamical meteorology to simplify balance equations, such as conservation equations [27]. The method is used to simplify the equation that contains at least three terms or for three variables [14].

Consider the three-term equation. For simplicity, the equation can be expressed as $S - M - N = 0$, where the three terms S , M , and N are all positive. Rewrite the equation as $S = M + N$. What the three-term equation implies is a balance of the larger term S by the two smaller terms M and N . Here, S is greater than both M and N in magnitude. By using the concept of scale analysis, it can be termed as “the scale of the S is larger than the scales of the M and N ”. With mathematic notation, this can be written as $O(S) > O(M)$ and $O(S) > O(N)$. In the present study, we examine the following two issues for the dominance in the three-term equation.

One is to find the dominant relation by simplifying the equation. Assume that M is much greater than N in magnitude, i.e., $O(M) \gg O(N)$. Then, we may ignore the small term N and simplify the equation of the three terms as $S \approx M$, a relation that describes a rough balance between the two dominant terms, the S and M . The other is to locate the dominant quantity when it is required to examine the variation of the smallest term N . Rewrite the equation as $N = S - M$. The N is a residual between S and M , the two larger terms. Here, the S has a positive effect and thus dominates the variation of the N . The M has a negative effect on the variation. For the specific issue of the relation of density, temperature, and pressure in this study, the differences of the magnitudes of A_D , B_T , and C_P may not be very large everywhere over the globe. However, the scale analysis is still pretty useful.

4.2. The Six Dominance Patterns and Their Geographical Preferences

In Section 3, for each pair of the quantities, the magnitudes of the corresponding terms in the equation are compared. The comparisons are all over the entire field. However, in different regions, the balance relation of the three terms may be dominated by different pairs of the quantities. In some regions, the relation can be simplified as the balance between density and temperature, while in other regions, the relation may be dominated by the balance between density and pressure or by the balance between temperature

and pressure. Here, for each grid point, we use the scale analysis introduced above to conduct the dominance examinations, i.e., to find the local relation dominated by two major quantities and their relative importance to the variation of the third quantity.

For examining the dominance, we may have three types (and further six patterns) through comparing the values of A_D , B_T , and C_P . Figure 4 shows the spatial distributions of these types and patterns. The three types are classified in terms of the smallest coefficient, from the A_D , B_T , and C_P . In Figure 4, the grid points with the C_P being the smallest, with the B_T being the smallest, and with the A_D being the smallest are marked in red, blue, and yellow, respectively. For each type, we may further divide it into two patterns in terms of the comparison of the other two coefficients. For example, for the type in red, with the C_P being the smallest, the grid points are further divided into the pattern with $B_T > A_D$, which is marked in dark red, and the pattern with $A_D > B_T$, which is marked in light red. The overall spatial distributions of these patterns for all the months in Figure 4 suggest that the patterns for the dominance possess significant geographical preferences.

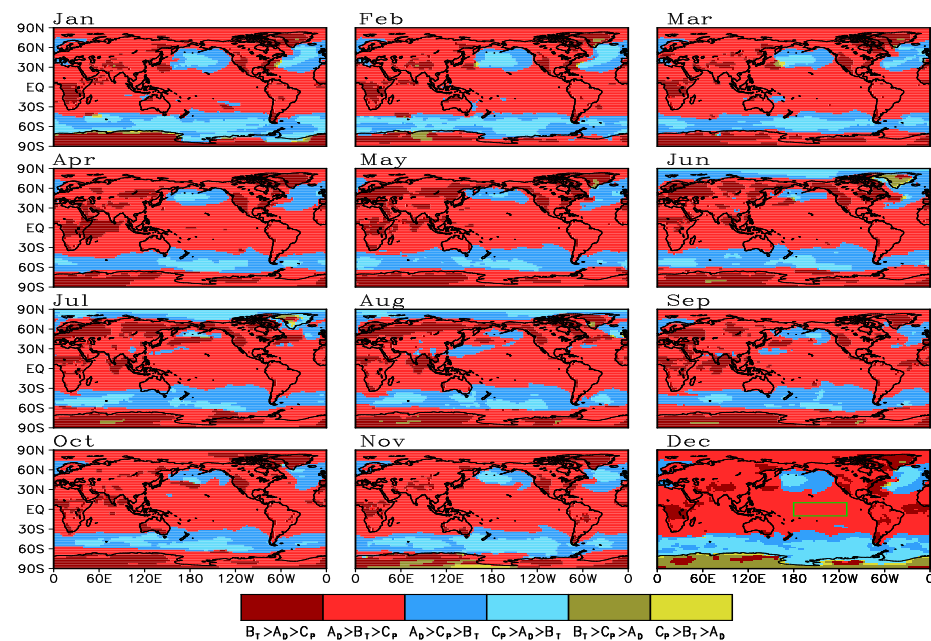


Figure 4. Geographical distributions of the three types (in red, blue, and yellow) and the final six patterns for dominance analysis in terms of the comparison among the coefficients A_D , B_T , and C_P . In the last plot for December, a region with the box marked in green is selected for use in Figure 5.

Table 1 presents the percentages of the grid points for the six patterns and the ratios of the grid points to the total over the globe. The percentages are provided for all the months, and their averages are used to assess the overall situation for the patterns. Over most grid points in the globe (75.7%; red), the type is the one with C_P being the smallest. Among them, the most popular pattern is the one with $A_D > B_T > C_P$ (61.5%; light red). Inside the wide regions of this pattern (Figure 4), there are some areas with the pattern of $B_T > A_D > C_P$ (14.2%; dark red). There is also a considerable number of grid points (23.1%; blue) where the type is the one with B_T being the smallest. They are mainly over the mid-high-latitude oceans in the two hemispheres. Within these regions, there are areas with the pattern of $A_D > C_P > B_T$ (15.5%; dark blue) and areas with the pattern of $C_P > A_D > B_T$ (7.6%; light blue). The grid points for the third type with A_D being the smallest (1.3%; yellow) are less and are major as the pattern of $B_T > C_P > A_D$ (1.1%; dark yellow). This pattern occurs mainly over Greenland in June and over Antarctica in December.

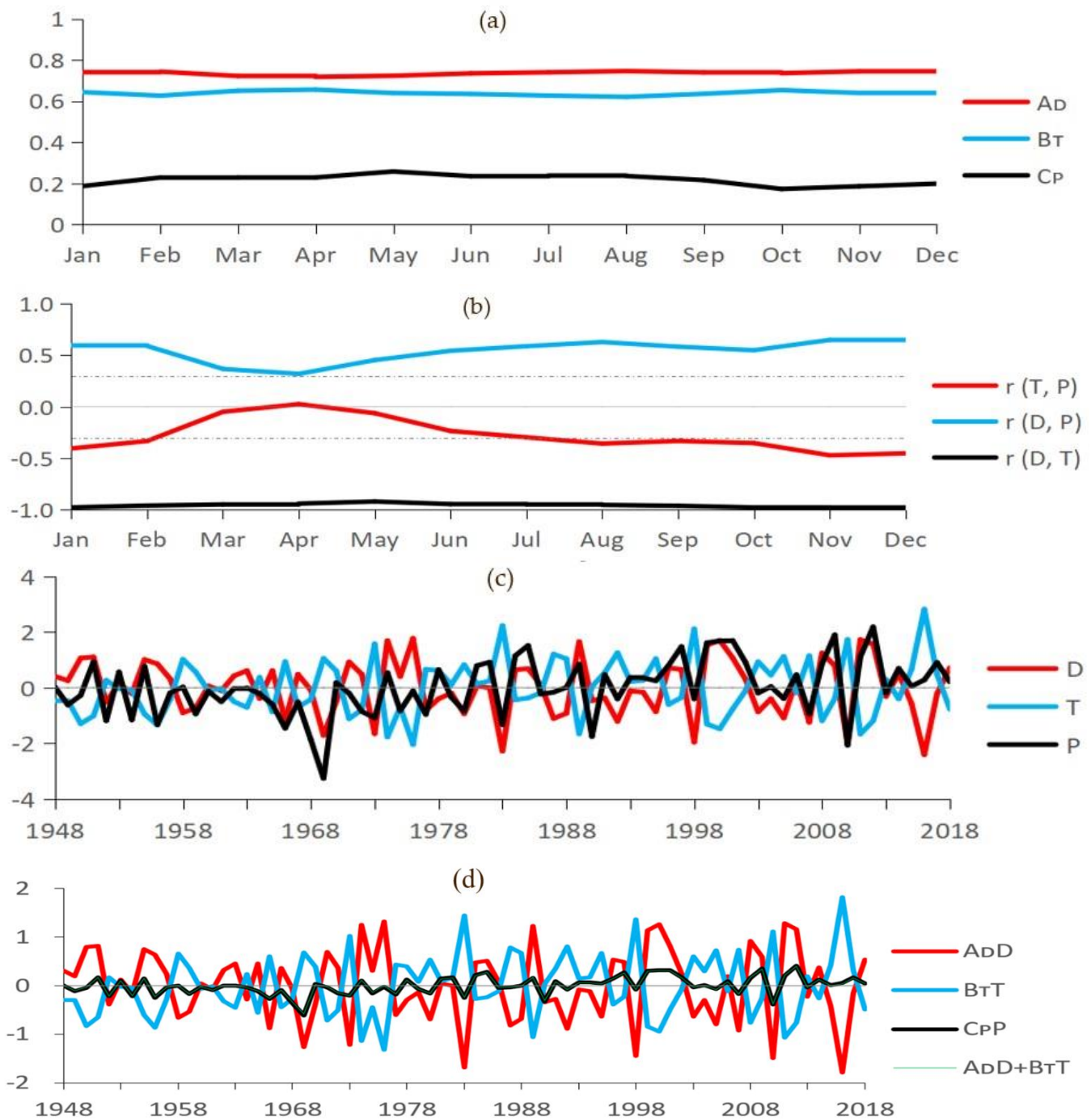


Figure 5. (a) The coefficients A_D , B_T , and C_P obtained for each month; (b) the correlation coefficients (r) between each pair of the normalized quantities (with the chain lines indicating the significance level of 0.01); (c) the year-to-year variations of the three normalized quantities D , T , and P for January; and (d) the corresponding variations of the $A_D D$, $B_T T$, $C_P P$, as well as the $A_D D + B_T T$. The curve for $A_D D + B_T T$ (green) overlies it for $C_P P$ (black). The data of pressure and temperature used for the calculations are averaged over the region selected in Figure 4.

For each of the six patterns, the scale analysis method can be applied to examine the two dominance issues. In the fitted plane equation $A_D D + B_T T - C_P P = 0$, as mentioned above, because of the normalizations, the three quantities D , T , and P are all in the magnitude of one. Or the scales of the three quantities are all equal to one, and this can be denoted as $O(D) = O(T) = O(P) = 1$. Then, the scales of the three terms A_D , B_T , and C_P

can be represented by the corresponding coefficients A , B , and C . With the notation, this can be expressed as $O(A_D D) = A$, $O(B_T T) = B$, and $O(C_P P) = C$.

Table 1. The ratio (unit: %) of the number of the grid points with each of the six patterns to the number of the total grid points over the globe.

Pattern	January	February	March	April	May	June	July	August	September	October	November	December	Mean
$B_T > A_D > C_P$ (Dark red)	14.7	9.1	12.8	14.4	17.0	16.6	18.3	17.3	16.4	14.7	9.8	9.1	14.2
$A_D > B_T > C_P$ (Light red)	58.3	66.6	66.3	65.9	62.5	55.2	54.9	56.3	64.4	66.2	64.6	56.4	61.5
$A_D > C_P > B_T$ (Dark blue)	14.0	13.4	14.4	15.8	17.0	19.7	16.8	18.0	17.0	14.7	13.8	11.3	15.5
$C_P > A_D > B_T$ (Light blue)	11.7	10.1	6.4	3.9	3.4	7.4	9.4	8.0	2.1	4.4	8.7	15.1	7.6
$B_T > C_P > A_D$ (Dark yellow)	0.8	0.7	0.2	0.0	0.1	0.8	0.5	0.4	0.2	0.0	2.5	6.9	1.1
$C_P > B_T > A_D$ (Light yellow)	0.5	0.1	0.1	0.0	0.0	0.2	0.1	0.1	0.0	0.0	0.5	1.2	0.2

For the most common pattern with $A_D > B_T > C_P$, which prevails over the wide regions marked in light red in Figure 4, the scale of the $C_P P$ is the smallest of the three terms. Actually, over these regions, the A_D and B_T are both much greater than the C_P in most of the grid points, as reflected in the plots of the A_D/C_P and B_T/C_P in Figure 3. That is, $C_P \ll A_D$ and $C_P \ll B_T$. As the first issue for the dominance, we may ignore the term $C_P P$ and simplify the equation as $A_D D + B_T T \approx 0$, representing a rough balance between the terms of the density and temperature. It can be inferred from this dominant relation that the D and T are negatively correlated. This means that corresponding to a larger-than-normal density, there might be a lower-than-normal temperature. As the second issue for the dominance, when examining the variation of the pressure, we rewrite the equation as $C_P P = A_D D - (-B_T T)$. This suggests that the small term $C_P P$ is the residual (i.e., the difference) between the two larger terms $A_D D$ and $-B_T T$. For this pattern with the $A_D > B_T > C_P$, we can also infer from the rewritten equation that the D is positively correlated with the P and thus dominates its variation. The T is negatively correlated with the P and has a negative effect on its variation.

The two patterns with the B_T being the smallest of the three, which appear over the northern Pacific, the northern Atlantic, and the ocean belt north of Antarctica, are also important. Similar to the above analysis, we may ignore the term $B_T T$, and simplify the relation as $A_D D - C_P P \approx 0$, a rough balance between pressure and density. The D and P may have a positive correlation. For the pattern with $C_P > A_D > B_T$, with the equation being rewritten as $B_T T = C_P P - A_D D$, the term $B_T T$ can be treated as the residual between the terms $C_P P$ and $A_D D$. Thus, pressure dominates the variation of the temperature, and density has a negative effect. For the pattern with $A_D > C_P > B_T$, we rewrite the equation as $B_T T = -A_D D + C_P P$, and the term $B_T T$ can be regarded as the residual between the terms $A_D D$ and $C_P P$. The variation of temperature is dominated by its negative correlation with density, i.e., the decrease in density, although the positive correlation with pressure can have a positive effect on the variation.

The A_D can also be the smallest of the three, and this is mainly for the pattern with $B_T > C_P > A_D$. This pattern appears mainly over Greenland in June and Antarctica in December. With neglecting the $A_D D$ and simplifying the equation as $B_T T - C_P P \approx 0$, the balance is between temperature and pressure. For the variation, we rewrite the equation as $A_D D = -B_T T + C_P P$ and conclude that the $A_D D$ is the residual between the terms $B_T T$ and $C_P P$. The variation of density is dominated by its negative correlation with temperature, i.e., the decrease in temperature, although the positive correlation with pressure can have a positive effect on the variation.

5. An Example with More Details from the Most Common Pattern

The most common pattern, with $A_D > B_T > C_P$, is taken as an example in this section. In the plot of December in Figure 4, a region with this pattern is selected and marked in green. The region lies in the central equatorial Pacific (110° W–180° W, 10° S–10° N). The pressure and temperature are averaged over the region. The density for the region is then calculated with the gas law. The plane fitting is performed for this region. Figure 5 presents

some more details of the pattern for the linear fitting, the scale analysis, and the results of the dominance.

Figure 5a presents the coefficients A_D , B_T , and C_P obtained for each month. Their values are pretty stable over the months. The A_D and B_T are comparable and large, while relatively the C_P is rather small. Thus, in the three-term equation, we may neglect the $C_P P$ and simplify the relation as a rough balance between the terms $A_D D$ and $B_T T$, i.e., $A_D D + B_T T \approx 0$. It can be inferred that D and T have different signs, suggesting that density and temperature are negatively related. Figure 5b shows that the correlation between D and T is truly negative, and it is very strong. The correlation coefficient can be almost -1.0 for all the months.

For examining the variation of the pressure, we rewrite the equation as $C_P P = A_D D + B_T T$. Comparison shows that A_D is greater than B_T in all months (Figure 5a). For a positive $C_P P$ in a year, we may infer from the equation that the $A_D D$ is positive, while the $B_T T$ is negative. This is consistent with the calculated results in Figure 5b, which indicates that pressure has a positive correlation with density but has a negative correlation with temperature. The $C_P P$ is thus a residual (or difference) between the two terms $A_D D$ and $-B_T T$. So, for this pattern, density dominates the variation of the pressure. Because of the dominance, the positive correlation of the pressure and density is strong. In contrast, temperature has a negative effect on the variation of the pressure.

With January being an example, Figure 5c displays the interannual variations of the three normalized quantities D , T , and P . They all have large year-to-year variations, and they are all in the magnitude of one because of the normalizations. Hence, the scales of the three terms $A_D D$, $B_T T$, and $C_P P$ can be measured simply with the corresponding coefficients A_D , B_T , and C_P . In addition, the curves can reflect the very strong negative correlation between the D and T , as well as the strong positive correlation between the P with D .

Figure 5d shows the interannual variations of the $A_D D$, $B_T T$, and $C_P P$, as well as the $A_D D + B_T T$. Here, the $C_P P$ corresponds to the pressure observed, and the $A_D D + B_T T$ is the $C_P P$ calculated with the fitted plane equation. In the plot, the curves of the $C_P P$ and the $A_D D + B_T T$ coincide exactly. This confirms the conclusion that for the gas law, a nonlinear relation, the plane fitting adopted in this study is perfect in linearizing the relation. We then may utilize the scale analysis method to assess the terms in the balance equation. The year-to-year perturbations of the $A_D D$ and $B_T T$ are truly large in scale, but they are opposite in sign. The $C_P P$ or the $A_D D + B_T T$ is small in scale and reflects the net effects of the terms $A_D D$ and $B_T T$. The $A_D D$ is greater than $B_T T$ in magnitude, thus $A_D D$ dominates the variation of the $C_P P$, and $B_T T$ has a negative effect on the variation.

6. Conclusions and Discussion

Dominance analysis is usually performed for the causal relation to find out the relative importance of the independent quantities to the dependent quantity. In this study, we examine the constraint relation with no causality and try to understand the dominance patterns in the relation.

Pressure, temperature, and density are important quantities for diagnosing the atmospheric circulation and the climate. For dry ideal gas, they are nonlinearly linked as the gas law. The relation is a simultaneous constraint. Although the three quantities are equal in position and they may all have changes regionally because of the interactions in the climate system, it is possible that one quantity does not change much, and the relation can be simplified as a balance between the other two quantities. In some regions, the relation may become Charles's law, with the density and temperature being inversely correlated. Over other regions, the relation may tend to be Boyle's law, with density and pressure being positively correlated, or Gay-Lussac's law, with temperature and pressure being positively correlated.

To be convenient for assessing the dominance, it is better to linearize the original nonlinear relation. For a general nonlinear problem, we use statistical fitting to linearize the relation. With the normalized quantities D , T , and P , the fitted plane equation can

be expressed as $A_D D + B_T T - C_P P = 0$, where $C_P > 0$, and $A_D^2 + B_T^2 + C_P^2 = 1$. Statistical tests indicate that the linearization is robust. Results show that corresponding to $C_P > 0$, the coefficients A_D and B_T are both positive everywhere. For this specific nonlinear problem, the gas law, the linearized relation can also be obtained from analytical derivations. Comparison indicates that the results are the same.

Scale analysis is a useful tool for simplifying equations that contain multiple terms. It has been applied in dynamical meteorology for analyzing conservation equations. Here, in the equation $A_D D + B_T T - C_P P = 0$, because of the normalizations, the quantities D , T , and P are all in the magnitude of one. So, the D , T , and P are actually the “dimensionless” variables for density, temperature, and pressure. Then, the coefficients A_D , B_T , and C_P can be regarded as the “scales” of the three quantities. Through comparing the scales, we examine two issues for the regional dominance. The first is to simplify the equation. After finding the smallest of the three scales, we may ignore the term and retain the other two terms in the equation. The second is to examine the variation of this term, which is the smallest in scale. The other two terms are opposite in sign but comparable in magnitude. Thus, the small-scale term we examine is a residual between the two large-scale terms. One of them dominates the variation, and the other has a negative effect on the variation.

For the dominance analysis, three types (and six further patterns) are obtained through comparing the three coefficients A_D , B_T , and C_P . The geographical distributions of the six patterns are provided for each of the months. The most common pattern is the one with $A_D > B_T > C_P$ (e.g., over the central equatorial Pacific), which appears over 60% of the grid points in the globe. The C_P is the smallest coefficient. In most of the regions, the C_P is actually much smaller than the A_D and B_T . So, in the equation, we may ignore the $C_P P$, and simplify the equation as $A_D D + B_T T \approx 0$. It is inferred that the D and T are opposite in sign and negatively correlated. When examining the variation of the pressure, we rewrite the equation as $C_P P = A_D D + B_T T$. Since $A_D > B_T$, it can also be inferred that $A_D D$ has a positive correlation with $C_P P$ and thus dominates the variation of the $C_P P$. The $B_T T$ has a negative effect on the variation. Hence, the $C_P P$ is a residual (or difference) between the terms $A_D D$ and $-B_T T$.

For the type with C_P being the smallest coefficient, another pattern is the one with $B_T > A_D$, which appears mainly over some land areas within the wide regions of the above pattern. The type with B_T being the smallest coefficient appears over the mid-high-latitude oceans in the two hemispheres. In the equation, we may ignore the $B_T T$ and simplify it as $A_D D - C_P P \approx 0$, suggesting a balance between the terms of pressure and density. The D and P can be positively correlated. The variation of the $B_T T$ can be analyzed with the equation $B_T T = C_P P - A_D D$. This type contains two patterns. For the pattern with $A_D > C_P$, the D and T are negatively correlated, and $-A_D D$ dominates the variation of $B_T T$, while $C_P P$ has a negative effect. For the pattern with $C_P > A_D$, $C_P P$ dominates the variation of $B_T T$, and $-A_D D$ has a negative effect on the variation. The type with A_D being the smallest coefficient, especially the pattern with $B_T > C_P$, may appear over some land areas in some months.

The example for the most common pattern displays many details on the plane fitting and the scale analysis. The quantitative results from this case examination are consistent with the results qualitatively inferred above from the fitting and the scale analysis. For instance, for this pattern with $A_D > B_T > C_P$, the linear fitting is perfect. The year-to-year curve of $C_P P$ from the observation and the curve of $C_P P$ from the fitted equation coincide exactly. The coefficients A_D and B_T are comparable, and they are truly much larger than the C_P . The normalized D , T , and P all have large interannual variations, although all in magnitude of one. The D and T have very strong negative correlation. The variation of the pressure is truly dominated by density, and the effect of temperature is negative.

For the linearized equation $A_D D + B_T T - C_P P = 0$, it is displayed that the spatial patterns of B_T and C_P , the scales of the terms of temperature and pressure, have significant seasonal shifts. The belts with small values of B_T and the belts with large values of C_P , which are over mid-high-latitude oceans in the two hemispheres, move northwards during

the first half of the year and southwards in the second half. This may be related to the seasonal movements of the incident solar radiation between the northern and southern hemispheres. This may be related to the storm tracks being located at slightly lower latitudes in winter than in summer. However, the spatial pattern of the A_D , the scale of the term of density, does not change much seasonally. Further investigations will be conducted to better understand these.

The task of the present study is to raise the question, propose the method, and locate the regions over the globe where the relation of the three quantities is dominated by the different types and patterns. It is the major finding of this study that the different dominance types and patterns have their geographical preferences. The two patterns with the C_P being the smallest of the three appear over most of the regions in the globe. The patterns with the B_T being the smallest appear over the northern Pacific, the northern Atlantic, and the ocean belt north of Antarctica. The patterns with the A_D being the smallest appear mainly over Greenland in June and Antarctica in December.

Atmospheric dynamics and physics will be investigated in our future work for the different types or patterns of the dominance in the relation. They are the final regional display, resulting from the dynamics and physics, as well as the interactions among the quantities. The investigation may also include the large-scale atmospheric circulation. This study needs to be conducted, individually, for each of the regions. The $B_T > A_D > C_P$ pattern, for example, appears over many land areas, including Antarctica, the Tibetan Plateau, South Africa, Eurasia, Greenland, and West America. For this pattern, the questions we may examine include why the variations of the temperature and density can offset each other and why the variation of the pressure is dominated by temperature rather than density. For the different land areas, the atmospheric circulation and physical processes responsible for the two questions can be different. For the pattern $B_T > C_P > A_D$, which only appears over Greenland in June and Antarctica in December, we may examine to find out what is special in the corresponding atmospheric circulations.

Water vapor is also an important quantity in real atmosphere. The relation among the pressure, temperature, density, and relative humidity (or other quantity that indicate moisture) is much more complex. The effect of the moisture will also be investigated in our future work. As a first step, we focus on the dry air in the present study and examine the dominance among pressure, temperature, and density, the three quantities for the dry air. We will consider the moist air through introducing a moisture quantity and then compare the relative importance of the moisture quantity with the dry-air quantities. Over the different regions of different dominance patterns, we may identify whether the variation of the moisture can be more important than the variations of the dry-air quantities or one or two of them.

Author Contributions: Conceptualization, E.L.; Data curation, J.T.; formal analysis, J.T. and E.L.; investigation, J.T. and E.L.; methodology, E.L.; software, J.T.; visualization, J.T.; writing—original draft, J.T.; writing—review and editing, D.Y. All authors have read and agreed to the published version of the manuscript.

Funding: This study was funded by the National Natural Science Foundation of China (grant 41991281), the National Key Research and Development Program of China (grant 2018YFC1507704), and the Priority Academic Program Development of Jiangsu Higher Education Institutions (PAPD).

Data Availability Statement: The NCEP Reanalysis Derived data used in this study were provided by the NOAA/OAR/ESRL, which are available at the site <https://www.esrl.noaa.gov/psd/> (accessed on 1 January 2022).

Acknowledgments: This study was supported by the National Natural Science Foundation of China (grant 41991281), the National Key Research and Development Program of China (grant 2018YFC1507704), and the Priority Academic Program Development of Jiangsu Higher Education Institutions (PAPD). The surface air temperature and pressure used in this study were obtained from the NCEP Reanalysis Derived data provided by the NOAA/OAR/ESRL PSD, Boulder, Colorado, USA, from their Web site at <https://www.esrl.noaa.gov/psd/> (accessed on 1 January 2022).

Conflicts of Interest: The authors declare no conflict of interest.

References

1. Budescu, D.V. Dominance analysis: A new approach to the problem of relative importance of predictors in multiple regression. *Psychol. Bull.* **1993**, *114*, 542–551. [[CrossRef](#)]
2. Azen, R.; Budescu, D.V. The dominance analysis approach for comparing predictors in multiple regression. *Psychol. Methods* **2003**, *8*, 129–148. [[CrossRef](#)]
3. Lu, E.; Takle, E.S.; Manoj, J. The relationships between climatic and hydrological changes in the upper Mississippi River basin: A SWAT and multi-GCM study. *J. Hydrometeorol.* **2010**, *11*, 437–451. [[CrossRef](#)]
4. Lu, E.; Ding, Y.; Zhou, B.; Zou, X.; Chen, X.; Cai, W.; Zhang, Q.; Chen, H. Is the interannual variability of summer rainfall in China dominated by precipitation frequency or intensity? An analysis of relative importance. *Clim. Dyn.* **2016**, *47*, 67–77. [[CrossRef](#)]
5. Tu, J.; Lu, E. Relative importance of water vapor and air temperature in the interannual variation of the seasonal precipitation: A comparison of the physical and statistical methods. *Clim. Dyn.* **2020**, *54*, 3655–3670. [[CrossRef](#)]
6. Lu, E.; Hao, J.; Yang, K. Temporal–Spatial Variations of Atmospheric Static Stability: A Comparison of the Influences from Temperature and Its Vertical Difference. *J. Clim.* **2021**, *34*, 4661–4674. [[CrossRef](#)]
7. Zumdahl, S.S. *Chemical Principles*; Houghton Mifflin Company: New York, NY, USA, 1998.
8. Grömping, U. Estimators of relative importance in linear regression based on variance decomposition. *Am. Stat.* **2007**, *61*, 139–147. [[CrossRef](#)]
9. Golub, G.H.; Van Loan, C.F. An analysis of the total least squares problem. *SIAM J. Numer. Anal.* **1980**, *17*, 883–893. [[CrossRef](#)]
10. Hoppe, H.; Derose, T.; Duchamp, T.; McDonald, J.; Stuetzle, W. Surface reconstruction from unorganized points. *ACM SIGGRAPH Comput. Graph.* **1992**, *26*, 71–78. [[CrossRef](#)]
11. Markovsky, I.; Van Huffel, S. Overview of total least-squares methods. *Signal Process.* **2007**, *87*, 2283–2302.
12. Cohen, J.; Cohen, P.; West, S.G.; Aiken, L.S. *Applied Multiple Regression/Correlation Analysis for the Behavioral Sciences*; Routledge: New York, NY, USA, 2013.
13. Bao, H. Accuracy comparison and analysis of three kinds of point cloud data plane fitting methods. *Geomat. Spat. Inf. Technol.* **2018**, *41*, 206–208.
14. Strahan, R.F. On the Nonintuitive Nature Of the Correlation Coefficient: Subjective Estimation of Three-Variable Relations. *Multivar. Behav. Res.* **1979**, *14*, 115–123. [[CrossRef](#)]
15. LaPorte, R.E.; Voss, J.F. Prose representation: A multidimensional scaling approach. *Multivar. Behav. Res.* **1979**, *14*, 39–56. [[CrossRef](#)]
16. Barenblatt, G.I. *Scaling, Self-Similarity, and Intermediate Asymptotics: Dimensional Analysis and Intermediate Asymptotics*; Cambridge University Press: Cambridge, UK, 1996.
17. Ding, C.S. Profile analysis: Multidimensional scaling approach. *Pract. Assess. Res. Eval.* **2001**, *7*, 16.
18. Cox, T.F.; Cox, M.A.A. *Multidimensional Scaling*; Chapman and Hall: London, UK, 2001.
19. Peixoto, J.P.; Oort, A.H. *Physics of Climate*; American Institute of Physics: New York, NY, USA, 1992.
20. Overland, J.E.; Bond, N.A. Observations and scale analysis of coastal wind jets. *Mon. Weather Rev.* **1995**, *123*, 2934–2941. [[CrossRef](#)]
21. Yano, J.-I.; Bonazzola, M. Scale analysis for large-scale tropical atmospheric dynamics. *J. Atmos. Sci.* **2009**, *66*, 159–172. [[CrossRef](#)]
22. Fullick, P. *Physics*; Heinemann Educational Books-Secondary Division: London, UK, 1994.
23. Levine, I.N. *Physical Chemistry*; University of Brooklyn, McGraw-Hill Co.: New York, NY, USA, 1978.
24. Crosland, M.P. The origins of Gay-Lussac’s law of combining volumes of gases. *Ann. Sci.* **1961**, *17*, 1–26. [[CrossRef](#)]
25. Gordon, A.H. Seasonal changes in the mean pressure distribution over the world and some inferences about the general circulation. *Bull. Am. Meteorol. Soc.* **1953**, *34*, 357–367. [[CrossRef](#)]
26. Brenner, I.S. Arizona cool season surface wind and pressure gradient study. *Bull. Am. Meteorol. Soc.* **1980**, *61*, 114–120. [[CrossRef](#)]
27. Holton, J.R. *An Introduction to Dynamic Meteorology*, 3rd ed.; Academic Press: New York, NY, USA, 1992.
28. Nigam, S.; Chan, S.C. On the summertime strengthening of the Northern Hemisphere Pacific sea level pressure anticyclone. *J. Clim.* **2009**, *22*, 1174–1192. [[CrossRef](#)]
29. Forsythe, G.E. A generalization of the thermal wind equation to arbitrary horizontal flow. *Bull. Am. Meteorol. Soc.* **1945**, *26*, 371–375. [[CrossRef](#)]
30. Dickson, R.R. A case study of the jet stream. *Bull. Am. Meteorol. Soc.* **1955**, *36*, 195–203. [[CrossRef](#)]
31. Mori, Y. A study on climatological aspects of winds in Japan. Part II: Mean fields of the thermal wind. *J. Clim.* **1988**, *1*, 143–156. [[CrossRef](#)]
32. Zhang, Y.; Yan, P.; Liao, Z.; Huang, D.; Zhang, Y. The winter concurrent meridional shift of the East Asian jet streams and the associated thermal conditions. *J. Clim.* **2019**, *32*, 2075–2088. [[CrossRef](#)]
33. Jung, C.; Schindler, D. The role of air density in wind energy assessment—A case study from Germany. *Energy* **2019**, *171*, 385–392. [[CrossRef](#)]
34. Ulazia, A.; Sáenz, J.; Ibarra-Berastegi, G.; González-Rojí, S.J.; Carreno-Madinabeitia, S. Global estimations of wind energy potential considering seasonal air density changes. *Energy* **2019**, *187*, 115938. [[CrossRef](#)]
35. Ren, D.; Dickinson, R.E.; Fu, R.; Bornman, J.F.; Guo, W.; Yang, S.; Leslie, L.M. Impacts of climate warming on maximum aviation payloads. *Clim. Dyn.* **2019**, *52*, 1711–1721. [[CrossRef](#)]

36. Hines, C.O. Gravity Waves in the Atmosphere. *Nature* **1972**, *239*, 73–78. [[CrossRef](#)]
37. Leal Iga, J.; Leal Iga, J.; Leal Iga, C.; Flores, R.A. Effect of air density variations on greenhouse temperature model. *Math. Comput. Model.* **2008**, *47*, 855–867. [[CrossRef](#)]
38. Kalnay, E.; Kanamitsu, M.; Kistler, R.; Collins, W.; Deaven, D.; Gandin, L.; Iredell, M.; Saha, S.; White, G.; Woollen, J. The NCEP/NCAR 40-year reanalysis project. *Bull. Am. Meteorol. Soc.* **1996**, *77*, 437–472. [[CrossRef](#)]

Disclaimer/Publisher’s Note: The statements, opinions and data contained in all publications are solely those of the individual author(s) and contributor(s) and not of MDPI and/or the editor(s). MDPI and/or the editor(s) disclaim responsibility for any injury to people or property resulting from any ideas, methods, instructions or products referred to in the content.